SSC-31

SSC-31

Superconducting Super Collider Laboratory

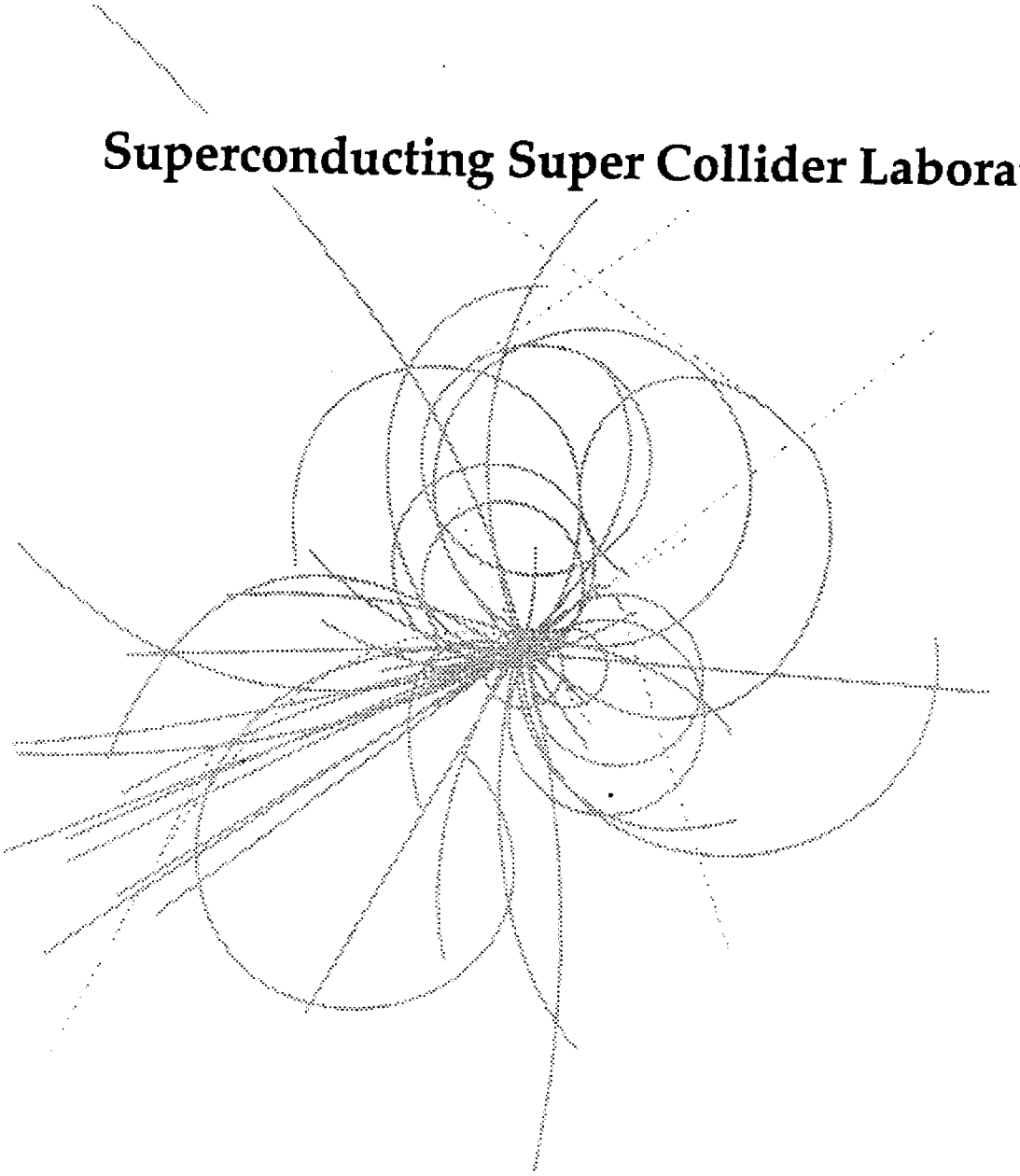

Accelerator Physics Studies for the SSC

A. Chao

April 1985

ACCELERATOR PHYSICS STUDIES FOR THE SSC*

A.W. Chao
Supercollider, URA Design Center†
c/o Lawrence Berkeley Laboratory, MS 90-4040
Berkeley, California 94720

In the spring of 1984, a reference designs study (RDS) was carried out to identify the issues and to provide a crude cost estimate of the SSC. [1] Following the RDS, a Central Design Group was formed in October to perform the detailed design R&D for construction of the SSC. This paper is a brief review of progress made on the accelerator physics studies since October 1984. For major issues not discussed here, many of them of great importance, the RDS report is still the valid source of information.

Three Types of Apertures

The most urgent accelerator physics issue identified in the RDS is the aperture evaluation because it translates directly to the magnet design and consequently its cost. Figure 1 shows schematically three types of apertures. The "physical aperture" is basically defined by the vacuum chamber of the beam channel. The "dynamic aperture" is an effective aperture of particle motion, beyond which the particle motion becomes unstable due to the nonlinear magnetic fields. The "linear aperture" is a new notion we introduced for the SSC aperture study; [2] inside this aperture, particle motion is basically linear, allowing the operational understanding of beam behavior. An ideal design is such that the physical aperture is slightly larger than the dynamic aperture, which in turn is slightly larger than the linear aperture.

The evaluation of the dynamic aperture requires the most extensive effort, which includes the developing and applying of the various analytic and particle tracking tools. (See a later section). Due to the intrinsic complexity of the nonlinear dynamics involved, however, the most dependable tool so far is the particle tracking codes. Given the lattice design and the nonlinear magnetic field errors, these tracking codes follow the particle motion for many (1,000, say) revolutions. By varying the launching amplitude of the particle being simulated and examining its stability, a dynamic aperture is obtained. This technique has the disadvantage that it provides only an upper limit of the dynamic aperature. It is not clear whether the aperture will shrink appreciably if the number of revolutions is increased (to 10^6, say).

The notion of a linear aperture is then introduced for two reasons. (1) The particle motion inside this aperture is basically linear, which means the motion is most likely stable. The linear aperture therefore gives a lower limit of the dynamic aperture. (2) During the operation stage, it is of great importance that the beam behaves according to what the linear theory predicts. A large linear aperture must be an important ingredient in the SSC design.

To quantify the linear aperture in a comprehensive manner, a set of criteria has been proposed, helped by the Tevatron operational experience. [2] In particular, inside the linear aperture, the tune variation with amplitude is not to exceed 0.005. Also, the variation of amplitude (action) from revolution to revolution should not exceed 10%.

The Nonlinear Magnetic Field Errors

The magnetic field error is of course one of the primary inputs to the aperture evaluation. One way to specify the field errors is through the harmonic expansion

$$B_y+iB_x = B_o \sum_{n=o}^{\infty} (b_n+ia_n)(x+iy)^n \qquad (1)$$

An ideal dipole magnet, for example, has $b_o=1$ and all other a_n and b_n coefficients vanish. For a magnet whose coil radius is r, the value of a_n and b_n of a crude magnet is roughly

$$a_n,\ b_n \sim \frac{1}{nr^n} \qquad (2)$$

For the SSC, however, we must do better than (2). To reduce the magnet cost, r needs to be made as small as possible (thus strong nonlinearities), while maintaining adequate aperture for beam stability and operation. To achieve that, sophisticated magnet designs have been initiated [3, 4, 5] and the work is continuing. Table 1 [6] shows the tentative field errors for one of the high field (6 tesla) cosθ magnet designs and for the low field (3 tesla) superferric design.

Table 1. Systematic/random field errors for one of the cosθ magnet designs and a superferric magnet design (tentative only). Unit: $[a_n] = [b_n] = 10^{-4}cm^{-n}$

	cosθ	Superferric
b_1	0/0.73	0/1.0
a_1	0/0.73	0/3.0
b_2	-1.3/2.7	2.3/1.0
a_2	0/0.73	0/1.0
b_3	0/0.5	0/0.5
a_3	0/0.8	0/2.0
b_4	0.65/0.7	-1.9/0.4
a_4	0/0.15	0/0.5
b_5	0/0.06	0/0.2
a_5	0/0.3	0/1.0
b_6	-0.17/0.085	2.0/0.5
a_6	0/0.047	0/0.4
b_8	0.9/0.035	0.16/0.3
b_{10}	0.0/0.015	0.0/0.0

To get a feeling on the tolerable level of nonlinearities, a rough "brick wall" criterion can be imposed: [7]

$$\beta\theta_B \sqrt{N_B}\ \left(\frac{\Delta B}{B}\right) < A, \qquad (3)$$

where β is the average betatron function, θ_B is the bending angle of a dipole magnet, N_B is the total number of dipole magnets, ΔB/B is the rms relative field error seen by a particle of betatron amplitude A. Using typical SSC values in (3), a rough rule of thumb is obtained: a particle that experiences a ΔB/B of the order of 5×10^{-4} around

*SSC-31

† Operated by Universities Research Association for the Department of Energy.

the ring is most likely unstable, while a linear motion would correspond to $\Delta B/B$ of the order of 5×10^{-5}. If we require a dynamic aperture of 1 cm, for example, the tolerable values of b_n's and a_n's are less than a few times $10^{-4}cm^{-n}$. Some of the coefficients in Table 1 are marginal in the sense and most likely need to be improved. As a particular example, the systematic b_8 coefficient (18-pole) of the cosθ magnet was found to restrict the dynamic aperture significantly. [8] The values of b_2's in Table 1 are also of concern. They probably either need to be better corrected or their effects be reduced by magnet sorting (shuffling) during installation. Various sorting schemes are currently being studied.

Test Lattices

The second primary input to aperture evaluation is the lattice design. The sensitivity of particle motion to nonlinearities depends critically on the lattice of the storage ring. The sensitivity of the tune values in the presence of nonlinear resonances is of course well known. In addition, the designs of the interaction region and the normal cells are also important factors. A useful aperture evaluation must take both the magnet errors and the lattice optimization into account.

To initiate the aperture evaluation and the selection of a basic magnet design, we have designed 8 basic test lattices. [9]

Table 1 SSC Test Lattices.

Lattice	Bend Field	Phase Advance/Cell	Tune	Cell Layer
A1	6.5T, cosθ	60°	82.3	200m
A2	" "	90°	118.3	"
B1	5T, cosθ	60°	88.3	220m
B2	" "	90°	130.3	"
C1	3T, superferric	60°	106.3	290m
C2	" "	90°	157.3	"
D1	6T, cosθ	60°	85.3	200m
D2	" "	90°	124.3	"
D1S	" "	60°	166.3	100m
C1S	3T, superferric	60°	247.3	145m
D1 (clustered IR)	6T, cosθ	60°	82.3	200m
C1 (clustered IR)	3T, superferric	60°	103.3	290m

These lattices are made as nearly identical as possible so that the various magnet designs, together with their respective field errors, can be evaluated as equally as possible. All 8 basic test lattices have 6 fold symmetry. Figure 2(a) shows schematically the test lattice structure for one sextant around each interaction point.

The β-functions at the interaction point is chosen to be $\beta_x^*=\beta_y^*=1m$ for the test lattices. This value however is not meant to be finalized. A smaller β* would mean higher luminosity (or equivalently, lower beam intensity for a given luminosity). The nonlinear chromatic effects associated with lower β* might be tolerable because of the relatively small energy aperture (10^{-3}) required of the beam. Whether this is indeed the case is a subject to be studied.

The normal cells have either 60° or 90° phase advance per cell. This allows well defined sextupole positions in the cells. In these test lattices, we have used the simplest scheme, i.e., two families of sextupoles to set the linear chromaticities to zero. Again due to the small needed energy aperture we have not yet seen the need of sophisticated multiple sextupole families to control the chromatic nonlinearities, although the possibility is not ruled out. Since the phase advance per cell is fixed, tune variations in the test lattices are obtained by adjusting the phase trombones. [9]

In Table 2, we have listed 4 more test lattices. The D1S and C1S lattices are similar to D1 and C1, except that the cell lengths are halved to study the optimization of cell structures (more in a later section). There are also 2 test lattices with clustered interaction regions of the C1 and D1 varieties. See Fig. 2(b). The C1S and D1S lattices are part of the aperture evaluation effort. The clustered IR lattices are to study the various accelerators physics and systems issues of the clustered IR's.

The test lattices have ignored such details as beam crossing geometry and utility sections. These details are not critical as far as nonlinearities are concerned and thus the test lattices are adequate for aperture evaluation purposes. We have also initiated an effort to develop the "realistic" lattices (starting with the lattices of the RDS) hopefully taking into account of all known details for accelerator systems purposes.

Aperture Studies

As mentioned before, aperture evaluation requires an extensive effort in both analytic and particle tracking studies. On the side of analytic studies, the conventional perturbation theory has been followed to derive the phase space invariant curves of the nonlinear Hamiltonian system. Given the lattice and the nonlinear field errors, this calculation gives an estimate of the maximum and minimum amplitudes (actions) a particle reaches as it circulates around the storage ring (to first order in the strength of nonlinearities). If the maximum amplitude of a certain particle is found to reach the physical aperture (vacuum chamber wall), the minimum amplitude of this particle is then interpreted as the dynamic aperture. Tools that provide this perturbation calculation have been developed. [10, 11] A parallel calculation in second order gives the variation of tunes with betatron amplitudes and energy deviation.

In addition to the conventional perturbation theory, there are other variations of the perturbation theory which also provides the invariant curves. These include the Deprit algorithm, [12] the superconvergency technique [13] and the iterative solution of the Hamilton-Jacobi equation. [13] Compared with the conventional perturbation theory, these approaches allow the calculation of the invariant curves be systematically carried to higher orders. Progress has been made by the respective authors in developing tools using these techniques, but at present they are not yet ready for the SSC applications.

Another analytic tool is the Lie algebraic approach. [14] One difference from the other approaches is that the Lie approach is most conveniently (although not fundamentally restricted to) expressed in a power series expansion in the canonical coordinates of particle motion. The perturbation parameter is therefore particle amplitudes

rather than the strength of nonlinearities. One disadvantage is that a high multipole field cannot be easily accommodated. For example, a field error $b_n x^n$ is of order (n-1) in the Lie approach while it is of the first order in the conventional perturbation language. Nevertheless, the Lie approach offers the complete information on the nonlinear maps of the storage ring to a specified order and the present tool, MARYLIE, can deal up to octupole order. A "normal form" technique has been developed [15] to extract information on the invariant curves and the tune variations up to the octupole order from the calculated nonlinear map.

The presently available analytic tools are most useful in fact not to find the dynamic aperture but to find the linear aperture. The tune variation with amplitude and momentum, $\Delta\nu$, is a direct product of the analyses. The variation of amplitude (action) $\delta A/A$ is easily obtained from the invariant curves in the phase space. (As mentioned before, linear aperture requires $\Delta\nu<0.005$ and $\delta A/A<10\%$). More importantly, the perturbation techniques are believed to hold best if the motion is almost linear.

As an example of the analytic work for the SSC, it has been estimated [11] that random sextupoles with rms $b_2=2\times10^{-4}cm^{-2}$ (no other field errors and without magnet sorting) give rise to a linear aperture of about 1 cm. This result agrees quite well with that obtained using the brick wall criterion [7] mentioned before.

We now turn to particle tracking efforts. Basically, four programs are being used and developed for the SSC: MARYLIE [14], DIMAT, [16] PATRICIA, [17] and PATRIS. [18] For example, MARYLIE is being extended to 10-th pole order with synchrotron oscillation capacity already available; PATRICIA and PATRIS are adding the possibility of simulating orbit distortions; and ways to symplectify DIMAT and PATRICIA have been studied and some incorporated in the codes. [19, 20]. At the time being, these code developments are still in progress and most of the tracking results so far are obtained by using the previous versions, especially of DIMAT and PATRICIA. There will be a review of the new code developments in July.

Although tracking obviously also yields information on the linear aperture, its most important application is to determine the dynamic aperture for a given lattice and given set of magnet field errors. Figure 3 shows the dynamic aperature results for the A1 and A2 test lattices using DIMAT and PATRICIA, which agree quite well with each other.

Figure 3 indicates that the systematic field errors severely reduced the dynamic aperture. However, the apertures achieved ($0.5\sqrt{2}$ mm for A1 and $0.7\sqrt{2}$ mm for A2 at the IP, corresponding to an aperture of 1.3 cm for A1 and 1.8 cm for A2 in the cells) are still adequate, admitting that random errors are not yet included. In addition, the field errors can still be improved and the cell structure of the lattices have not been optimized.

In terms of field errors, it was shown [8] that the 18-pole has been doing most of the damage in reducing the aperture. By artificially switching it off, the dynamic aperture doubles. In terms of optimizing the cell structure, the severe reduction of aperture by multipole errors is a strong indication that the cell length has been chosen too long. The nonlinearities have basically two sources: those associated with the bare lattice and those associated with multipole field errors. The two contributions scale very differently with the cell length of the lattice. An optimal cell length is obtained when these two sources of nonlinearities contribute equally in restricting dynamic aperture. [21]

Figure 4 [22] is the expected behavior of the dynamic aperture for A1 and A2 lattices due to the two sources of nonlinearities. The optimum half cell lengths, according to Fig. 4, are determined by the intersection points of the dotted and the solid lines, i.e. 60 m for A2 and 35 m for A1, for the particular set field errors used. The optimum dynamic aperture in both cases will then be approximately $0.9\sqrt{2}$ mm at the IP. For this reason, we have initiated the short cell test lattices discussed in Table 2. It needs to be pointed out here that a shorter cell length means higher cost because of the need of more quadrupole magnets.

Figure 5 shows the dynamic aperture for the case of C1 lattice using the superferric magnet errors of Table 1. [23] In this case, only the random multipoles (no systematic multipoles) are included. In the absence of multipole errors, the on-momentum aperture is found to be $7.7\sqrt{2}$ mm at IP. With multipole errors, aperture is found to be $0.24\sqrt{2}$ mm, representing a reduction factor of 30. A shorter cell version of C1 will also be developed to study the dependence of aperture on cell length for the superferric magnets.

In all tracking studies mentioned above, we have made tune scans in the neighborhood of the working point. In all cases, it is found that the dynamic aperture does not vary much (~10%) in a region of tune space covering $\Delta\nu_{x,y} = \pm0.01$.

For a given magnet design, the multipoles scale with the magnet coil size roughly as a_n, $b_n \propto r^{-(n+1)}$. Larger coil size means smaller multipoles and thus larger dynamic aperture. In Ref. 23, it was found that the dynamic aperture increases by 40% when the coil size is increased by 20%. The penalty of course is that magnets with larger coil size cost more.

Much more work needs yet to be done. Tracking with both random and systematic multipoles, checking the dependence of dynamic aperture on the cell length and inclusion of orbit distortion effects [24] are just a few more obvious examples. After these, iterations with the magnet designers and cost estimators will become important. For a given detailed magnet design and with the needed aperture (both dynamic and linear apertures) specified, [2] the optimization procedure is to find the cell length and the magnet coil radius that minimize the cost of the storage ring. This indeed is a challenge we have yet to meet.

Collective Effects

In the RDS, an optimization procedure that involved the luminosity, the beam emittance and the number of events per collision had yielded the needed beam intensity of about 1.5×10^{10} per bunch and a spacing of 10-15 m between adjacent bunches in each beam. These results are still the nominal valves used for evaluation of collective effects.

Collective effects relate to the aperture requirements in two ways. First, the longitudinal and transverse impedances that cause beam instabil-

ities depends on the physical aperture of the vacuum chamber size. A small vacuum chamber gives higher impedances and therefore lower threshold beam intensity against instabilities. Second, in order for the beam to be stable, it needs to have a minimum energy spread, which in turn imposes a condition on the energy aperture of the lattice.

It is expected that the impedance of the SSC comes mainly from bellows, pick-up electrodes and resistive wall (4°K copper) of the vacuum chamber pipe, and the rf cavities to a lesser extent. To allow for thermal contraction from room temperature to 4°K, 1.2% of the storage ring circumference is occupied by bellows. The bellows are therefore assumed to be shielded. A careful itemized estimate of the impedance for a 6 Tesla ring gives [25] a longitudinal impedance of $Z_{||}/n = 0.35\Omega$ and a transverse impedance of $Z_{\perp} = 50$ M Ω/m. For the 3 tesla ring, it is estimated to have basically the same $Z_{||}/n$ but $Z_{\perp}$ is larger by a factor of 1.4 to 1.7, depending on details of the estimation.

For the SSC, the primary source of single bunch beam instability is that caused by the mode coupling (i.e., fast head-tail) effect. This instability can be cured by having sufficient energy spread in the beam particles. The needed energy spread is related to the transverse impedance and the number of particles in the bunch, N, by [25]

$$\frac{\sigma_E}{E} = \frac{1}{8\pi^{3/2}F} \frac{e^2 c\beta Z_{\perp} N}{\eta E R} \qquad (4)$$

where F is a form factor of the order of 1, β is the betafunction at the impedance, η is the momentum compaction factor, R is the average radius of the ring. For the 6 tesla test lattices, eq. (4) gives $\sigma_E/E = 6\times10^{-5}$ and 9.5×10^{-5} for D1 and D2 lattices, respectively.

The needed σ_E/E for beam stability scales with the ring size according to $\sigma_E/E \propto \beta Z_{\perp}/\eta R$. For the test lattices, we have approximately $\beta \propto \sqrt{R}$, $\eta \propto 1/R$. Since R doubles from the 6 tesla case to the 3 tesla case, the needed σ_E/E increases by a factor of 2.0 to 2.4. Furthermore, the vacuum chamber pipe radius is taken to be 33 mm. The 3 tesla option of reducing the pipe radius to 25 mm would result in an even higher value of σ_E/E by a factor of 1.7 to 2.0. Then the needed σ_E/E becomes $2\text{-}4\times10^{-4}$.

To accommodate the rf noise problem, it is suggested to have a 3 to 1 bucket to bunch area ratio. The rf bucket height is then 4 times σ_E/E. For the case of 3 tesla and 25 mm pipe radius, the rf bucket height would be up to the level of $1\text{-}2\times10^{-3}$, which is very close to the energy being achieved by the aperture test lattices.

Both longitudinal and transverse multi-bunch instabilities are expected to play roles. [25] Damping with broad-band feedback systems is foreseen. The requirement on a longitudinal feedback system is expected to be somewhat easier for the 3 tesla case, while the requirement on the transverse system would be slightly more difficult. In either case, no severe limitations are discovered.

Beam-Beam Effects

Although the beam-beam perturbation is one of the primary source of nonlinearities, we have not yet included it in our aperture evaluation, partly because it is not expected to directly impact on the selection of the basic magnet design. However, we have paid attention to providing enough stable tune space in the test lattices for the beam-beam purposes. In addition, we have studied the overlap knockout effect and the effect of coherent dipole instabilities caused by the long-range beam-beam collisions.

The overlap knockout instability occurs when the revolution frequencies of the two beam are slightly different and when a resonance condition (see equation (5) later) is approximately satisfied. [26] The frequency difference can be a result of a difference in the circumferences of the two rings, orbit distortions or when the two beams have different energies for operational purposes during injection with beams separated.

It is possible to avoid frequency split by locking the rf systems. But in order to operate the two beams with different energies during injection for example, this requires the two beams to have energy error of $\pm1\text{-}5\times10^{-3}$, [26] which is wasteful in terms of the available energy aperture of the lattice.

For the SSC, taking into account of the facts that the superperiod is 6 and that each beam consists of many bunches with bunch spacing D, the dipole overlap knockout resonances occur at

$$\nu - 6n = \frac{\delta C}{D} k \qquad (5)$$

where ν is the betatron tune, δC is the equivalent circumference difference, n and k are integers.

If the beams are operated at different energies during injection procedure, $\delta C \approx 6$ cm. Taking D=15 m, the resonances are densely populated in ν space, i.e., $\nu-6n=\pm0.004k$. A calculation [27] assuming a beam separation of 5 mm and 26 long range encounters per interaction region has yielded Fig. 6, which shows the contribution to the effective beam emittance from the overlap knockout resonances. The emittance growth even away from resonances is found to be large compared with the natural emittance of 10^{-9} m at 1 TeV. However, the resonance strength decreases with increasing order k. By operating sufficiently away from ν=6n, the overlap knockout may become tolerable. In addition, a broad band feedback system can be activated. Whether the tune spread (which is comparable to the resonance spacing) will make things difficult is yet to be studied.

The circumference difference δC due to surveying error or due to horizontal closed orbit distortions are to be compensated by the locking of rf systems in order to assure the interaction point does not drift during collisions. Since the associated energy deviations are restricted to $<10^{-3}$, there is a upper limit on δC which is estimated to be <2 cm. Note that δC represents the relative difference in the two circumferences and not the absolute errors.

Study of the coherent dipole instability due to the large number of bunches (10^4) and the long range beam-beam interaction between the two beams has been started. The bunches move as rigid charge distributions in model so far. The corresponding dipole instability occurs when the betatron tune ν is close to integers. The study so far has not used the SSC parameters but already indicated that the long range interactions do substantially increase the stopband widths around the integer resonances for the SSC crossing angle (30-100 μrad). The inclusion of multipole coherent instabilities will

create resonances when ν is close to a rational number and it is important to know as the next step if the stopbands corresponding to these multipole modes are not increased too much by the long range collisions.

References

[1] SSC Reference Designs Study, May 8, 1984.

[2] D. Edwards, SSC Aperture Task Force Interim Report - the Aperture Criterion Group, SSC-22, April 1985. This is to be supplemented by T.L. Collins, On Choosing an Aperature, SSC-26, April 1985 and M. Harrison, Tevatron Operational Experience and Implications for SSC Aperture, SSC-27, April 1985.

[3] E. Fisk, these proceedings.

[4] R. Huson, these proceedings.

[5] P. Reardon, these proceedings.

[6] E. Fisk and J. Peterson, SSC Aperture TAsk Force Report - the Magnet Errors Group, SSC-7 (1985).

[7] S. Peggs, M. Furman, A. Chao, A Possible Screening Procedure for Random Multipole Field Errors, SSC-20, April 1985.

[8] B.T. Leemann, D.R. Douglas, E. Forest, these proceedings, SSC-24 (1985).

[9] E.D Courant, D.R. Douglas, A.A. Garren and D.E. Johnson, these proceedings, SSC-19 (1985).

[10] C. Leemann, SSC Aperture Task Force Intermin Report - the Analytic Screening Group, to appear as SSC report, April 1985.

[11] S. Heifets, Random Sextupoles in the SSC Lattice, SSC-21, April 1985.

[12] L. Michelotti, these proceedings.

[13] R. Ruth and R. Warnock, talks presented in the Aperture Task Force review meeting, April 22-23, 1985, work in progress. Also, these proceedings.

[14] A. Dragt, High Energy Accelerator Summer School, Fermilab, 1981, AIP Proc. No. 87, p. 147.

[15] E. Forest, Normal Form Algorithm on Non-Linear Symplectic Maps, SSC-29, April 1985.

[16] R.V. Servranckx and K.L. Brown, SLAC-PUB-270 (1984).

[17] H. Wiedemann, Private communications, work in progress, 1985.

[18] A. Ruggiero, private communications, work in progress, 1985.

[19] M. Furman, Simple Method to Symplectify Matrices, SSC-6, 1985.

[20] D.R. Douglas, E. Forest and R.V. Servranckx, these proceedings.

[21] R. Talman, et. al., Ann Arbor Workshop on Accelerator Physics Issues for a SSC, 1983, UM HE 84-1, p. 28.

[22] S. Peggs, talk presented in the Aperture Task Force Review meeting, April 22-23, 1985, to appear as SSC report.

[23] G. Dell, talk presented in the Aperture Task Force Review meeting, April 22-23, 1985.

[24] K. Lau, preliminary results presented in the Aperture Task Force Review meeting, April 22-23, 1985.

[25] J. Bisognano, Collective Effects and the Design of the SSC, these proceedings.

[26] S. Myers, Overlap Knockout Resonances in the SSC, SS-14 (1985).

[27] A. Chao and C. Leemann, More on the Overlap Knockout Resonances in the SSC, SSC-16 (1985).

[28] A. Chao and J. Peterson, Internal Note SSC-N-7 (1985).

[29] M. Furman and A. Chao, these proceedings.

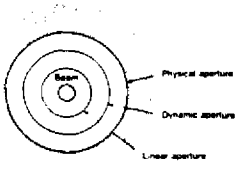

Fig. 1 Schematic of three types of aperture.

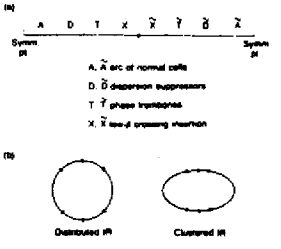

Fig. 2 (a) Structure of the basic test lattices for one sextant around each interaction point. The lattice is anti-symmetric about the IP and the symmetry points. (b) distributed IR and clustered IR test lattices.

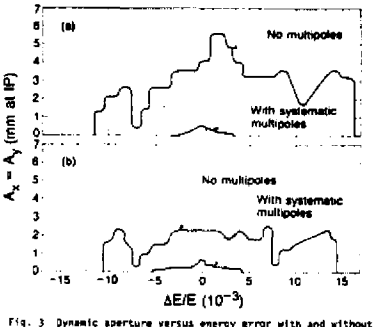

Fig. 3 Dynamic aperture versus energy error with and without the systematic multipole field errors. Both figures are without random field errors. The aperture is given as A_x and A_y at the interaction point where β^*=1m. No synchrotron oscillation is included. The dynamic aperture is obtained by requiring stability for 40" revolutions. (a) for the A1 test lattice, (b) for the A2 lattice.

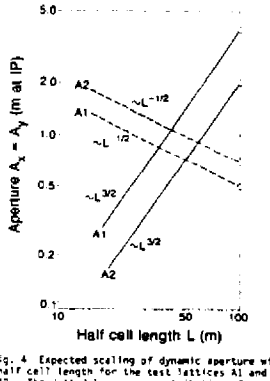

Fig. 4 Expected scaling of dynamic aperture with half cell length for the test lattices A1 and A2. The dotted lines are contributions from multipole field errors. The solid lines are contributions from the bare lattice. The four circled points are obtained from the on-momentum values of Fig. 3

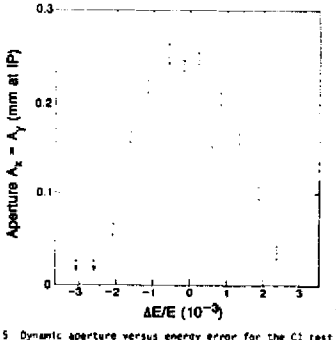

Fig. 5 Dynamic aperture versus energy error for the C1 test lattice. Random multipoles errors are included but the systematic multipoles are not.

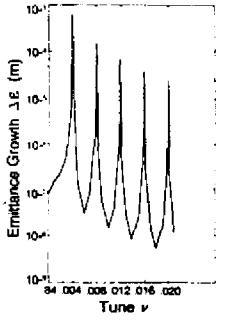

Fig. 6 Effective emittance growth due to overlap knockout resonances.